Steel and Composite Structures, *Vol. 22, No. 1 (2016) 63-77*
DOI: http://dx.doi.org/10.12989/scs.2016.22.1.063

Stress-transfer in concrete encased and filled tube square columns employed in top-down construction

Sun-Hee Kim [1a], Kyong-Soo Yom [2] and Sung-Mo Choi [*1]

[1] *Department of Architectural Engineering, University of Seoul, Cheonnong-dong 90, Dongdaemun-Gu, Seoul, 130-743, Republic of Korea*
[2] *Harmony Engineering, Guro-Gu Seoul 152-051, Republic of Korea*

(*Received June 09, 2016, Revised September 07, 2016, Accepted September 11, 2016*)

Abstract. Top-down construction is a construction technique in which pit excavation and structure construction are conducted simultaneously. Reducing construction time and minimizing noise and vibration which affect neighboring structures, the technique is widely employed in constructing downtown structures. While H-steel columns have been commonly used as core columns, concrete filled steel tube (CFT) columns are at the center of attention because the latter have less axial directionality and greater cross-sectional efficiency than the former. When compared with circular CFT columns, square CFT columns are more easily connected to the floor structure and the area of percussion rotary drilling (PRD) is smaller. For this reason, square CFT columns are used as core columns of concrete encased and filled square (CET) columns in underground floors. However, studies on the structural behavior and concrete stress transfer of CET columns have not been conducted. Since concrete is cast according to construction sequence, checking the stress of concrete inside the core columns and the stress of covering concrete is essential. This paper presents the results of structural tests and analyses conducted to evaluate the usability and safety of CET columns in top-down construction where CFT columns are used as core columns. Parameters in the tests are loading condition, concrete strength and covering depth. The compressive load capacity and failure behavior of specimens are evaluated. In addition, 2 cases of field application of CET columns in underground floors are analyzed.

Keywords: concrete encased and filled square (CET) column; welded built-up square column; loading condition; concrete stress transfer; pre-load; core column

1. Introduction

Although H-steel columns have been commonly used as core columns, CFT columns are emerging as new core column members because their less axial directionality and higher cross-sectional efficiency make them more structurally and economically desirable. When compared with circular CFT columns, square CFT columns are more easily connected to the floor structure and the area of percussion rotary drilling (PRD) is smaller. The use of CFT columns as the core columns of CET columns simplifies construction process and improves cross-sectional efficiency (Kim *et al*. 2011, Lee *et al*. 2013). If square CFT columns are installed as underground core

∗Corresponding author, Professor, E-mail: smc@uos.ac.kr
[a] Research Professor
[b] President

http://www.techno-press.org/?journal=scs&subpage=6 ISSN: 1229-9367 (Print), 1598-6233 (Online)

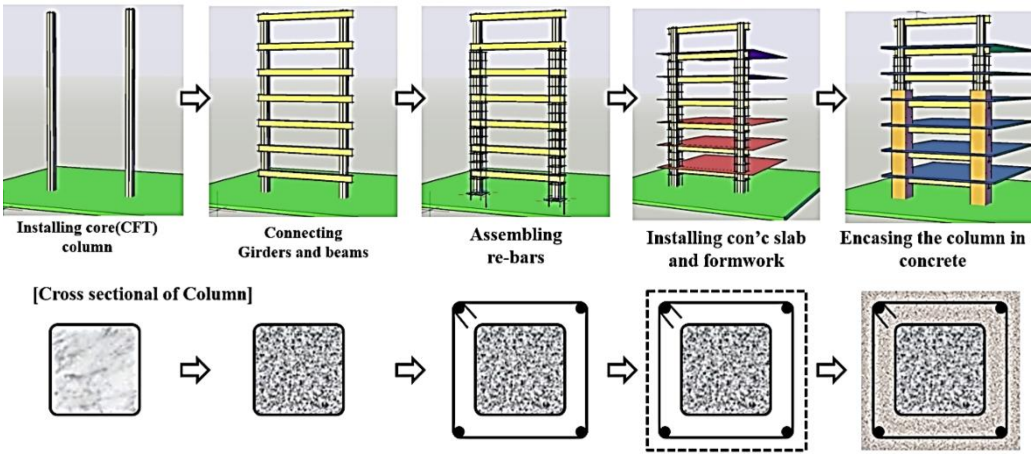

Fig. 1 Construction sequence & column cross-section

columns and concrete is cast for encasing afterwards, it is possible to conduct partial construction in accordance with applied load. It is also possible to use only CFT columns on the upper floors above the ground and to cover the columns on lower floors with concrete to ensure required level of structural performance (Kim *et al*. 2013). Since concrete is cast according to construction sequence as shown in Fig. 1, the cross-sections of the columns vary. Therefore, both the stress of the concrete inside the core columns and that of covering concrete should be evaluated. The concrete inside the core column resists construction load in cooperation with the steel tube and part of the load is transferred to the covering concrete which is cast afterwards. There are no design/construction guidelines to decide whether stress is properly assigned according to the load and whether the core column and the covering concrete can be treated as a single medium. Studies on the structural performance of CET columns need to be conducted from different perspectives. Less than required reference information about concrete stress is available. In this study, structural tests were conducted to evaluate the usability and safety of square CFT columns used as the core columns of CET columns in top-down construction. Specimens were fabricated for the analysis of load capacity and failure behavior with parameters of loading condition, concrete strength and covering depth.

2. Previous studies on CET columns

Tsuda and Matsui (1987) analyzed the failure behavior and load capacity of general steel tube columns, CFT columns and CET columns subject to compressive force. Parameters in the test were shape (square and circular) and width-thickness ratio (b/t: 25~138). The result of the study suggested that significant difference in concrete stress-strain relationship between CFT columns and CET columns resulted from concrete confinement effect.

Park (2011) analyzed the behavior and strength of steel-concrete composite circular columns with confinement effect taken into consideration. His test and analysis found that design standard for circular CFT and CET compression members underestimated the improvement in strength resulting from concrete confinement effect. It was also found that the strength and moment of CET compression members increased when concrete covering depth increased but only the core columns resisted load after the separation of covering concrete.

Seon (2010) conducted static loading tests on CFT columns and CET columns and analyzed load-displacement relationship and failure behavior. The load capacity of CET columns increased linearly in the initial stage of elasticity as in the case of reinforced concrete columns, but they showed ductile behavior after yielding. In addition, strength improved when width-thickness ratio was 25~50.

More studies and tests have been conducted on CET columns. However, they focused on how to prevent the covering concrete from falling or compared the compressive load capacity of CET columns with that of CFT columns. In other words, studies on CET columns centered on cross-sectional efficiency and concrete confinement effect in comparison with CFT columns. No studies have been conducted on the concrete stress of CET columns during construction. The load capacity of CET columns at each stage of construction sequence is not evaluated and reflected in designs. Since more than half of accidents occur during construction (KBC-2009), it is essential to check concrete stress at each stage.

3. Experimental program

3.1 Test overview

5 specimens were fabricated as shown in Table 1. Parameters in the tests were loading condition, concrete strength and covering depth. As shown in Fig. 2, welded built-up CFT columns were used as core columns. 4 steel plates were bent and welded at the centers of 4 sides to avoid stress concentration in corners. The width of the core columns was 160 mm and the thickness of the steel was 3.2 mm. The width-thickness ratio (b/t) of the steel tubes was 48 and the yield strength (F_y) of the steel was 325 MPa. Since the width-thickness ratio was smaller than the limit of 56.7 ($2.26\sqrt{E/F_y}$), the columns had compact sections. The total width including covering was 340 mm and the area of covering was 89,558 mm^2. In the core column, steel area (As) and concrete area (Ac) were 2,346 mm^2 and 23,165 mm^2, respectively. The AISC-2010 Specification Chapter I requires that steel area in a CFT column should be more than 1% of total area. Steel area was 2.03% of the total area in the specimens. Fig. 3 shows graphic description of the specimens.

In the field, core columns are constructed with constant load applied. In order to reflect the

Table 1 Specimen list

No.	Name	B_{inner}	t_{inner}	L	B_{outer}	A_{s_tube}	A_{r_bar}	A_{c_CFT}	$A_{c\_protect}$	Preload
	Unit	mm	Mm	mm	Mm	mm²	mm²	mm²	mm²	kN
1	1_30_90	160	3.2	560	340	2,346	163	23,165	89,558	-
2	1_50_90	160	3.2	560	340	2,346	163	23,165	89,558	-
3	2_30_90	160	3.2	560	340	2,346	163	23,165	89,558	571.01
4	2_50_90	160	3.2	560	340	2,346	163	23,165	89,558	767.91
5	2_50_110	160	3.2	560	360	2,346	163	23,165	118,358	767.91

2-50-90
→ Covering depth(mm)
→ Concrete Strength of Pre-founded column(MPa)
→ 1: Uniform Load , 2: Preload +Uniform load

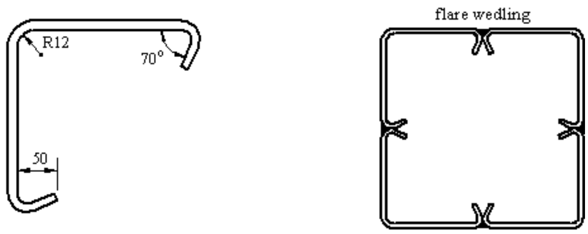

Fig. 2 Core column shape (welded built-up section)

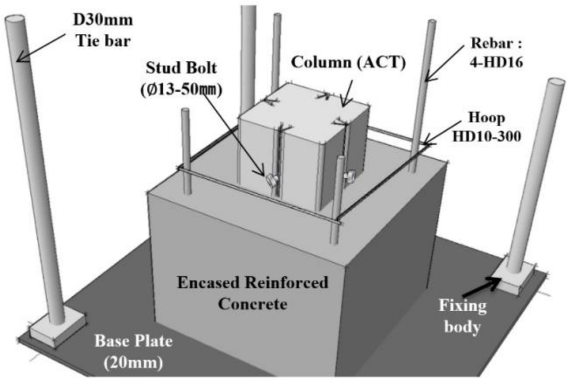

Fig. 3 Specimen concept

field condition, tie bars which were 30 mm in diameter were installed at the 4 corners of the base plate and 50% of the core column’s available compressive strength was pre-loaded. Available compressive strength was estimated by Eq. (1) as prescribed in the AISC-2010 Specification. Design strength was employed as material strength in the equation. For example, 571 kN was preloaded to specimen 2-30-90 because available compressive strength was 1,142 kN.

$$P_{n0} = F_y A_s + F_{ysr} A_{sr} + 0.85 f_{ck} A_c \tag{1}$$

Taking into consideration tensile force applied to each tier bar, screw heads which were 50 mm in diameter were welded to the upper plate. In addition, wedge-shaped anchoring devices were attached at the bottom ends of the tie bars in order to minimize slip. 3 stud bolts (Ø13-50 mm) were placed in a low in side faces of the column for integration with the concrete.

3.2 Loading and stress flow

In order to realize boundary condition at the core column, the column was covered with concrete after constant load was applied. Uniformly distributed load was applied to the CET column for the analysis of load capacity and behavior. Fig. 4 explains the 4 steps of the test. Step 1) Concrete was cast in the steel tube and cured. Step 2) Tie bars were anchored at 4 corners and preload was applied through the bars. Since the core column was subject to load, the bars were anchored not to disturb tensile force. Step 3) Concrete was cast into the mold which was placed around the column and cured. Step 4) Uniform load was applied by a 980kN UTM. Specimen 2

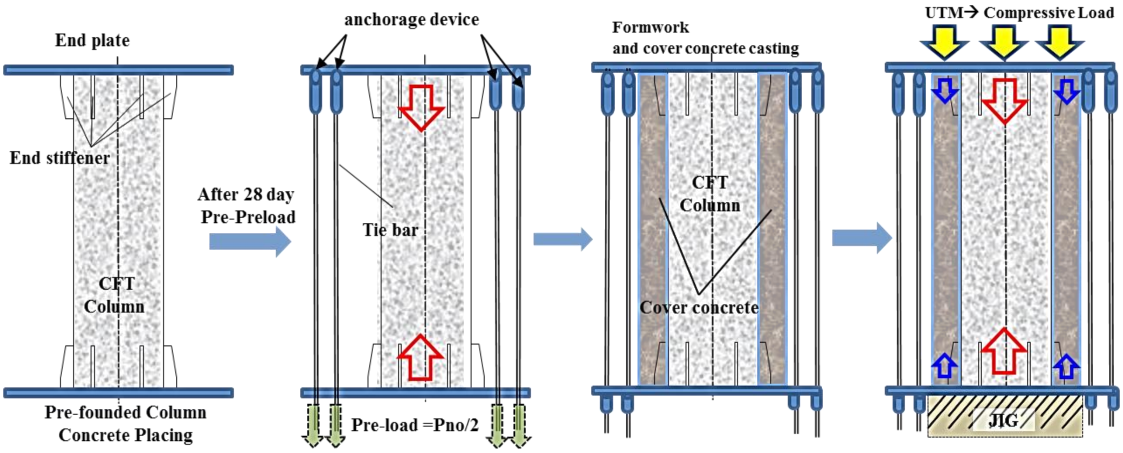

(a) Step 1 (b) Step 2 (c) Step 3 (d) Step 4

Fig. 4 Stress flow

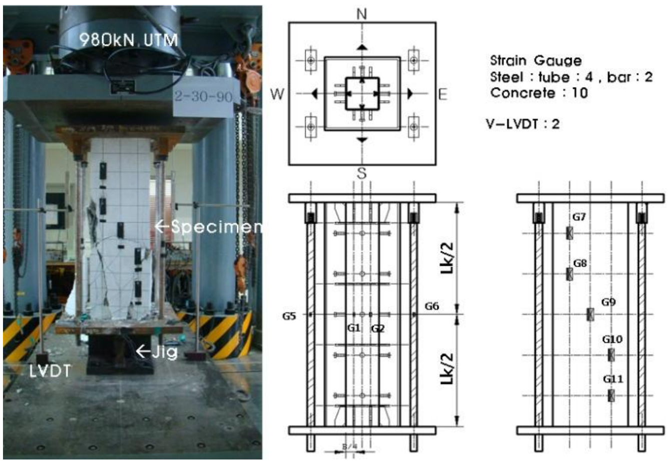

Fig. 5 Loading & measuring

and specimen 3 did not go through step 2.

3.3 Measurement

1-axis strain gauges were placed at the faces of the steel tube and the covering concrete as shown I Fig. 5 to observe deformation and behavior. 4 gauges were placed axially and horizontally avoiding the stud bolts attached to the steel tube of the core column. Strain gauges were also attached to the centers of the tie bars. A jig was placed on the movable platform in order to apply load to the specimen without the interference from the anchoring devices or rebars.

3.4 Material test

Coupon test was conducted on the 3.2 mm thick steel used in the specimens in accordance with

Table 2 Results of coupon test

No.	Area (mm^2)	Elastic modulus (GPa)	Yield strength (MPa)	Tensile strength (MPa)	Yield ratio	Elongation (%)
1	74.88	190	341	426	0.80	31%
2	74.46	198	353	447	0.79	33%
3	74.80	200	357	452	0.79	30%
AVE	74.71	196	350	441.67	0.79	31.3%

Table 3 Concrete compressive strength

No.	Compressive design strength -30 MPa		Compressive design strength -50 MPa	
	Test result (MPa)	Correction value (MPa)	Test result (MPa)	Correction value (MPa)
1	42.14	40.87	54.18	52.55
2	46.55	45.15	52.36	50.79
3	37.70	36.57	51.87	50.31
4	43.16	41.86	50.14	48.64
5	41.10	39.87	50.08	48.58
AVE	42.13	40.87	51.73	50.17

ASTM E08/E8M-11. Average yield strength (F_y) and tensile strength (F_u) of the steel were 350 MPa and 442 MPa, respectively.

Two types of concrete having design compressive strength of 30 MPa and 50 MPa were used. In order to evaluate compressive strength (f_{ck}), test pieces which were 100 mm in diameter and 200 mm in height were made. As shown in table 3, corrected values of average compressive strength obtained by the application of correction factor (0.97) were 41 MPa and 50 MPa, respectively.

4. Structural test results

4.1 Axial force-displacement relationship-

Monotonic load was applied until compressive strength declined to 80% of its maximum. Displacement was measured by LVDTs installed at both ends of the specimen. The specimens exhibited similar patterns of load-displacement relationship as shown in Fig. 6.

While compressive strength was higher in the specimens that were not preloaded, the differences were very slight, meaning that they had similar strength and stiffness levels. Table 4 shows ultimate compressive strength (Pu), displacement at failure (Pu_disp) and initial stiffness (k_i) of the specimens. The values of displacement at failure (Pu_disp) in the table are the values of the axial displacement of the whole column observed at the point of ultimate compressive strength.

4.2 Failure mode

Concrete cracking signaled deformation, which was followed by the deformation of rebars after yielding. Fig. 7(a) shows the failure of the specimens where load was applied to core columns and

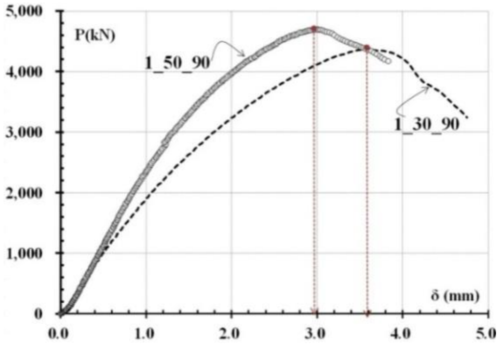

(a) ‘1’ series

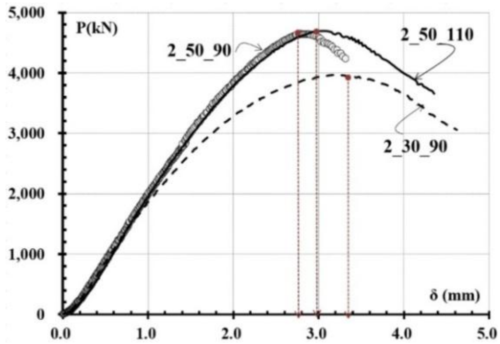

(b) ‘2’ series

Fig. 6 Axial force-displacement curve

Table 4 Ultimate compressive strength & initial stiffness

Name	P_u (kN)	P_{u_disp} (mm)	K_i (kN/mm)
1_30_90	4360.8	3.6	1816
1_50_90	4698.6	3.0	1853
2_30_90	3968.1	3.2	1832
2_50_90	4643.1	2.8	1832
2_50_110	4696.2	3.0	1827

(a) ‘1’ series specimens

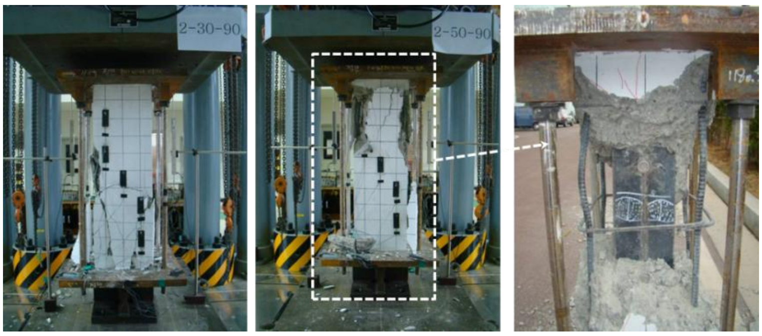

(b) ‘2’ series specimens

Fig. 7 Failure mode

covering concrete simultaneously without preloading. Concrete falling started from the upper parts of the specimens and cracking expanded to the lower parts after maximum load capacity was exhibited. After the test was terminated, remaining concrete was removed to confirm steel tube buckling. Local buckling was observed at the upper part of the steel tubes, which corresponded to the locations of severe concrete cracking.

In preloaded specimens, concrete cracking started throughout the faces and the deformation of rebars was aggravated after yielding and continued until maximum load capacity was exhibited. Local buckling was observed at the steel tubes of the specimens.

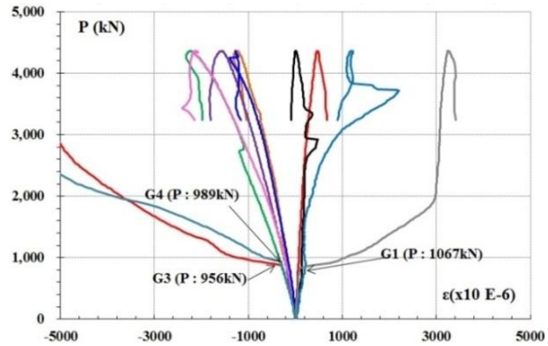

(a) 1_30_90

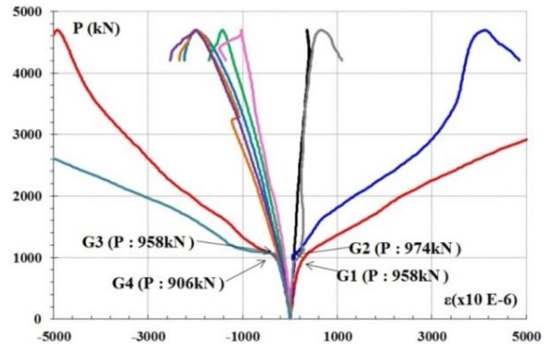

(b) 1_50_90

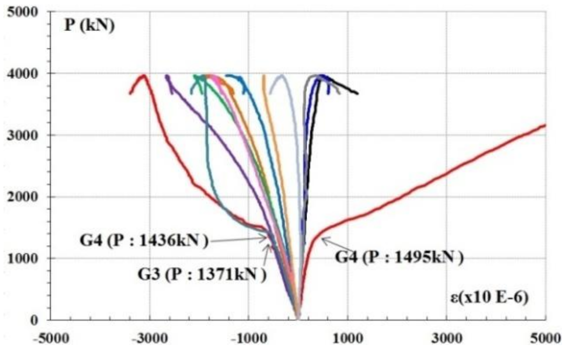

(c) 2_30_90

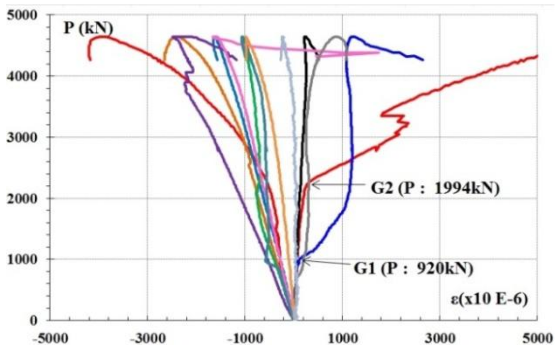

(d) 2_50_90

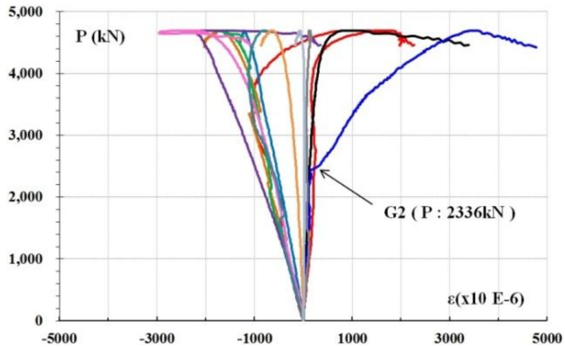

(e) 2_50_110

Fig. 8 Axial force-strain relationship

5. Analyses and findings

5.1 Axial force and strain relationship in core columns

4 strain gauges were mounted at the center of the core column (G1, G2: axially, G3, G4: perpendicularly to the axis). Fig. 8 shows axial force-strain relationship observed at the specimens.

The slopes of the lines obtained from the gauges mounted at the steel tubes change rapidly, suggesting the deformation (buckling) of the tubes at certain load. Table 5 compares compressive strength at steel tube deformation, available compressive strength and design compressive strength of core columns. The values of compressive strength at deformation were clearly identified at the test and the values corresponding to the first occurrence of deformation were used for the comparison. The values obtained from material test were used in Eqs. (2)~(4) (AISC-2010).

Compressive strength at the deformation of the core columns lies between available compressive strength and design compressive strength. Comparison of the 4 identically shaped specimens found that buckling strength was 121% of design compressive strength but only 60% of available compressive strength. It is deduced that load capacity lying between the core column's available compressive strength and design compressive strength indicates the possibility of steel tube deformation (buckling) and calls for re-evaluation of structural safety. In the specimen with covering depth of 110 mm, compressive strength at steel tube deformation was higher than available compressive strength and design compressive strength.

$$P_e = \pi^2 (EI_{eff})/KL^2 \tag{2}$$

When $\frac{P_{no}}{P_e} \leq 2.25$

$$P_n = P_{no}\left[0.658^{\frac{P_{no}}{P_e}}\right] \tag{3}$$

When $\frac{P_{no}}{P_e} > 2.25$

$$P_n = 0.877 P_e \tag{4}$$

As mention in Section 4.1, the difference in compressive strength between preloaded specimens and those without preloading was less than 5%. And, test results of core columns were compared

Table 5 Buckling strength results & estimated values (Unit: kN)

Specimen	P_ε	P_o	P_e/P_o	P_n	P_e/P_o
1_30_90	956	1535	0.62	840	1.14
1_50_90	906	1712	0.53	888	1.02
2_30_90	1371	1535	0.89	840	1.63
2_50_90	920	1712	0.54	888	1.04
2_50_110	2336	1712	1.36	888	2.63
Average (Excluding 2_50_110)			**0.64**		**1.20**

Table 6 Comparison between design values & test values

Name	$f_{ck\text{–inner}}$	Preload (kN)	P_{AISC2010} (kN)	P_{u_test} (kN)	P_{test} / P_{AISC2010}
1_30_90	30	0	4095.3	4360.8	1.06 (-0.06)
1_50_90	50	0	4272.5	4698.6	1.10 (-0.10)
2_30_90	30	571.01	4095.3	3968.1	0.96 (+0.04)
2_50_90	50	767.91	4272.5	4643.1	1.08 (-0.08)
2_50_110	50	767.91	5055.9	4696.2	0.93 (+0.07)

with the values obtained from design equations as mentioned in Section 5.1. This chapter presents comparison which was made between the values obtained from the design equations in the AISC-2010 Specification Chapter I and test values in order to determine whether the equations could be applied to CET columns. Since the CFT columns were produced and installed before they wore concrete covering, the factor (C1 or C3) needed for the estimation of effective stiffness in buckling strength Eq. (2) was adjusted from 0.9 to 0.3. Between Eqs. (3) and (4) for design compressive strength, the former was used because all of the specimens were of inelasticity.

5.2 *Test values vs. estimated values*

Table 6 summarizes test values and estimated values. Test values were lower than design values in 2 of the preloaded specimens. Test values were higher than design values in the specimens without preloading. However, the differences were within the range of ±10%.

5.3 Load capacity and concrete compressive strength

Concrete having higher compressive strength is usually cast in the steel tubes of core columns to reduce covering. The safety of the columns needs to be evaluated in relation to concrete strength. Table 7 summarizes the comparison of compressive strength values. Stiffness was not noticeably affected by concrete compressive strength. The differences in preload-free specimens and preloaded specimens were approximately 7% and 16%, respectively, both of which were higher than 4% estimated by the equation. Concrete area in the core column was less than 20% of the whole area and dealt with less than 5% of the overall load. Nevertheless, the compressive strength of the concrete in core columns exerted greater influence on the load capacity of the specimens than was expected. Since the amount of preload is determined by the load that the core column deals with, the improvement of load capacity can be achieved through the use of high strength material.

Table 7 Load capacity & concrete compressive strength

Specimen	P_{u_test} (kN)		Initial stiffness (kN/mm)		$P_{AISC2010}$ (kN)	
1_30_90	4360.8	1.07	1816	1.04	4095.3	1.043
1_50_90	4698.6		1653		4272.5	
2_30_90	3968.1	1.16	1832	1.01	4095.3	1.043
2_50_90	4643.1		1845		4272.5	

Table 8 Load capacity & covering depth

Specimen	P_{u_test} (kN)		P_{u_disp} (mm)	$P_{\_AISC2010}$ (kN)	
2_50_90	4643.1	1.011	2.8	4272.5	1.183
2_50_110	4696.2		3.0	5055.9	

Table 9 Load capacity and loading method

Specimen	P_{u_test} (kN)		Initial stiffness (kN/mm)		$P_{AISC2010}$ (kN)	
1_30_90	4360.8	0.91	1816	1.01	4095.3	1.00
2_30_90	3968.1		1832		4095.3	
1_50_90	4698.6	0.99	1653	1.11	4272.5	1.00
2_50_90	4643.1		1845		4272.5	

5.4 Load capacity and covering depth

Compressive strength was compared between two specimens shown in Table 8 to evaluate the influence of covering depth. While the equation estimated that the increase of covering depth from 90 mm to 110 mm would result in an 18% improvement in compressive strength, the test provided similar results of compressive strength and displacement between the two. It is deduced that the initial cracking of the covering concrete impeded load capacity. Although the relation between covering depth and load capacity was not clearly identified through the comparison between the 2 specimens, the accumulation of data involving a larger number of CET composite columns will provide quantitative analysis of the relation. It is suggested that improving coherence and adhesion between the concrete and rebars rather than increasing covering depth excessively is a more effective way to improve load capacity.

5.5 Load capacity and loading method

Axial load applied to the core column is transferred to the covering concrete. The influence of the load transfer mechanism on the concrete inside the steel tube and on the ultimate resistance force of the CET column was analyzed. Table 9 summarizes the result.

Compressive strength was higher in the specimens which were not subject to preload. When ultimate compressive strength and initial stiffness were non-dimensionalized, the difference associated with loading method was approximately 10%. This result is relevant when preload is less than 50% of the core column’s available compressive strength. In the specimens that were not preloaded, stress flowed throughout the whole sections from the beginning of loading. In the preloaded specimens, pre-stress was re-distributed after covering.

6. Field application of CET columns

In this chapter, field application of CET columns in actual buildings is analyzed. Table 10 shows the outline of the 2 cases of field application including building information and material properties. The buildings were designed by ultimate strength design method and completed in

Table 10 Outline of field application

Case 1) Bird's-eye view	Title		OOO Hall New Construction
	Location		Yeongdeungpo-Gu, Seoul in Korea
	Height		245 m (50 stories above ground 6 underground levels)
	Use		Office, Conference hall, retail shop
	Scale		Lot Area: 12,146 m^2 Gross floor area: 168,681 m^2
	Structure type		Steel-frame structure, RC structure
	Material property	Steel	SM490 (Fy:325MPa)
		Con'c	(1) CFT: 50 MPa; (2) CET(cover con'c): 30 MPa
		Re-bar	SD400 (Fy: 400 MPa): D32. D13
		Stud bolt	F10T (D16-@300)
Case 2) Bird's-eye view	Title		Alpha Dome city New Construction
	Location		Gyeonggi-do in Korea
	Height		61 m (15 stories above ground 7 underground levels)
	Use		Office, retail shop
	Scale		Lot Area: 89,040 m^2 Gross floor area: 33,053 m^2
	Structure type		Steel-frame structure, RC structure
	Material property	Steel	SM490 (Fy: 325 MPa)
		Con'c	(1) CFT: 49 MPa; (2) CET(cover con'c): 40 MPa
		Re-bar	SD500,600 (Fy: 500,600 MPa): D32. D13
		Stud bolt	F10T(D16-@300)

Table 11 Cross-sections of CET columns

	Case 1	Case 2
Cross section (N/mm^2 , mm)	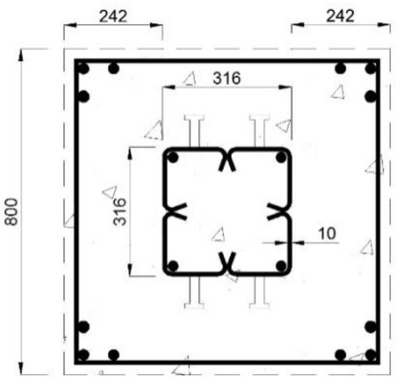 Center col.(CFT) Underground 1~6F: □-316×316×10 CET : Underground 1~6F: □-800×800	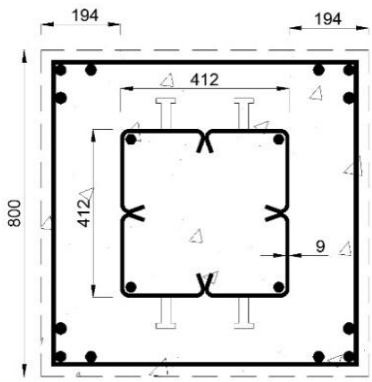 Center col.(CFT) Underground 1~7F: □-412×412×9 CET : Underground 1~7F: □-800×800

Table 11 Continued

Pn	CFT : 7,316 kN CET : 27,436 kN			CFT : 10,912 kN CET : 33,216 kN		
Pre-load ratio	FL	*Pu* (kN)	*Pu*/*Pn* (CET)	FL	*Pu* (kN)	*Pu*/*Pn* (CET)
	B1	3,569	**18%**	B1	4046	**18%**
	B2	5,886	**29%**	B2	4641	**21%**
	B3	8,653	**43%**	B3	5237	**23%**
	B4	9,908	**49%**	B4	5834	**26%**
	B5	11,296	**56%**	B5	6435	**29%**
	B6	12,688	**63%**	B6	7066	**32%**
	-	-	-	B7	7276	**33%**

2013 and 2016. CET columns were used in underground floors of the buildings. Table 11 shows the cross-sections and applied compressive strength (*Pu*) of the columns. The design compressive strength of the core (CFT) columns is 7316 kN and 10912 kN in case 1 and case 2, respectively. The design compressive strength of the concrete covering is 20,120 kN and 22,304 kN. The design compressive strength of the whole CET column was 1.36 and 1.49 times that of the concrete covering. The rate of applied compressive strength (*Pu*) to design compressive strength (*Pn*) on the lowest floor was 63% in case 1 and 33% in case 2. In the test, compressive strength was 121% of design compressive strength on average and preload ratio was 50%. It is suggested that employing CET columns in top-down construction with the load ratio and preload ratio will result in desired concrete stress flow.

7. Conclusions

Monotonic loading tests were conducted on CET column specimens with parameters of loading method, concrete strength and covering depth to evaluate the structural safety of the columns in different stages of construction sequence. The comparison between test results and estimated values indicated what should be considered in the design of CET columns. Although the findings in this study are not enough to quantitatively analyze the influence of the boundary conditions on load capacity, they can be used as the basic data for ensuring required structural performance.

- Difference in loading method did not result in noticeable differences in load capacity and structural behavior. Despite the absence of guidelines and design equations for this situation, the tests and analyses conducted in this study suggest that top-down construction using CET columns does not compromise structural safety. Design process including the amount of preload and details of rebar installation should be established to induce desirable results.
- The buckling strength of the core columns was between available compressive strength and design compressive strength. Structural safety should be re-evaluated if load capacity lies between available compressive strength and design compressive strength because the possibility of steel tube deformation exists.
- Increase in the strength of concrete inside the core columns resulted in a more than 10% increase in load capacity. It is deduced that using concrete of higher compressive strength

can be considered to improve load capacity because it affects preload amount and covering depth.

- Increase in covering depth did not result in noticeable changes in load capacity and displacement. The result suggests that improving coherence and adhesion between the concrete and rebars rather than increasing covering depth excessively is more effective in improving load capacity.
- Although load capacity was slightly higher when preload was not applied, buckling strength was similar regardless of loading method. It is deduced that stress was distributed throughout the whole section of the column from the beginning of loading when it was not preloaded, while pre-stress resulting from preloading caused the re-distribution of stress after covering.

References

AISC (2005, 2010), Steel Construction Manual; American Institute of Steel Construction Ins.

Fenollosa, E., Gil, E., Cabrera, I. and Vercher, J. (2015), "Elastic-plastic formulation for concrete encased sections interaction diagram tracing", *Steel Compos. Struct., Int. J.*, **19**(4), 861-876.

KBC (2005, 2009), Korean Building Code; Architectural Institute of Korea.

Kim, B.H., Sim, H.J., Choi, B.J. and Lee, E.T. (2011), "Flexural behavior of concrete filled seismic resistant steel tubular columns subjected to axial and cyclic lateral load", *J. Korean Soc. Steel Construct.*, **23**(3), 317-326. [In Korean]

Kim, S.H., Yom, K.S. and Choi, S.M. (2013), "Evaluation of the fire resistance performance of interior anchor type CFT columns through loaded heating test", *Int. J. High-Rice Build.*, **2**(1), 39-48.

Kim, S.H., Yom, K.S. and Choi, S.M. (2014), "Improving fire performance with steel-fibers for internally anchored square composite columns", *J. Construct. Steel Res.*, **103**, 264-274.

Kim, S.H., Yom, K.S. and Choi, S.M. (2015), "A study on the structural performance of new shape built-up square column under concentric axial load", *Steel Compos. Struct., Int. J.*, **18**(6), 370-377.

Ky, V.S., Tangaramvong, S. and Thepchatri, T. (2015), "Inelastic analysis for the post-collapse behavior of concrete encased steel composite columns under axial compression", *Steel Compos. Struct., Int. J.*, **19**(5), 1237-1258.

Lee, C.H., Kang, K.Y., Kim, S.Y. and Koo, C.H. (2013), "Review of structural design provisions of rectangular concrete filled tubular columns", *J. Korean Soc. Steel Construct.*, **25**(4), 389-398. [In Korean]

Li, N., Lu, Y.Y., Li, S. and Liang, H.J. (2015), "Statistical-based evaluation of design codes for circular concrete-filled steel tube columns", *Steel Compos. Struct., Int. J.*, **18**(2), 519-546.

Park, G.D. (2011), "Strength evaluations and behavior properties considering confined effects for steel composite circular columns", Doctorate Thesis; Inha University, Korea.

Seon, W.H. (2010), "Experimental study of strength and deformation behavior for CET column", M.S. Dissertation, Inha University, Korea.

Tsuda, K. and Matsui, C. (1987), "Structural performance and limiting width thickness ratio of concrete filled steel square tubular columns", Earthquake Engineering, New Zealand, August, pp. 25-36.

Xu, T., Xiang, T., Zhao, R. and Zhan, Y. (2010), "Nonlinear finite element analysis of circular concrete-filled steel tube structures", *Struct. Eng. Mech., Int. J.*, **35**(3), 315-333.

Zaharia, R. and Dubina, D. (2014), "Fire design of concrete encased columns: Validation of an advanced calculation model", *Steel Compos. Struct., Int. J.*, **17**(6), 835-850.

BU

Nomenclature

A_s	=	cross sectional areas of steel (mm^2) $(= A_{s,tube})$
A_c	=	cross sectional areas of concrete (mm^2)
$A_{c,CFT}$	=	cross sectional areas of concrete in steel tube (mm^2)
$A_{c,cover}$	=	cross sectional areas of cover concrete (mm^2)
A_r	=	cross sectional areas of reinforced bar (mm^2)
B_{inner}	=	width of steel tube column (CFT) (mm)
B_{Outer}	=	width of concrete covered column (CET) (mm)
EI_{eff}	=	Effective stiffness of composite section
E_c	=	Young's modulus of concrete (MPa)
E_s	=	modulus of elasticity of steel (200000 MPa)
F_u	=	Tensile strength of steel (MPa)
F_y	=	specified minimum yield stress of steel section (MPa)
F_{ysr}	=	specified minimum yield stress of reinforcing bars (MPa)
f_{ck}	=	Compressive strength of concrete (MPa)
L	=	laterally unbraced length of the member (mm)
t_{inner}	=	Thickness of steel tube (mm)
P_{no}	=	Available compressive strength (Eq. (1))
P_e	=	elastic critical buckling load determined in accordance with Eq. (2) (N)
EI_{eff}	=	Effective stiffness of composite section (N-mm^2) When encased composite compression member = $E_sI_s + 0.5E_sI_{st} + C_1E_cE_C$ When filled composite compression member = $E_sI_s + 0.5E_sI_{st} + C_3E_cE_C$
C_1	=	Coefficient for calculation of effective rigidity of an encased composite compression member $= 0.1 + 2(\frac{A_s}{A_c + A_s}) \leq 0.3$
C_3	=	Coefficient for calculation of effective rigidity of filled composite compression member $= 0.1 + 2(\frac{A_s}{A_c + A_s}) \leq 0.9$
I_c	=	moment of inertia of the concrete section about the elastic neutral axis of the composite section, (mm^4)
I_s	=	moment of inertia of steel shape about the elastic neutral axis of the composite section, (mm^4)
I_{sr}	=	moment of inertia of reinforcing bars about the elastic neutral axis of the composite section, (mm^4)
K	=	effective length factor